Perfect coupling of light to surface plasmons by coherent absorption

Heeso Noh, Yidong Chong, A. Douglas Stone, and Hui Cao*

Department of Applied Physics, Yale University, New Haven, Connecticut 06520, USA

(Received 29 September 2011; published 3 May 2012)

We show theoretically that coherent light can be completely absorbed and transferred to surface plasmons in a two- or three-dimensional metallic nanostructure by exciting it with the time-reversed mode of the corresponding surface plasmon laser (''spaser''). The narrow-band perfect absorption is a generalization and application of the concept of critical coupling to a nanocavity with surface plasmon resonances. Perfect coupling of light to nanostructures has potential applications to nanoscale probing as well as background-free spectroscopy and ultrasensitive detection or sensing.

DOI: 10.1103/PhysRevLett.108.186805 PACS numbers: 73.20.Mf, 42.25.Bs, 42.25.Hz

A fundamental issue in nanophotonics is the efficient delivery of light into regions with subwavelength dimension, to enhance linear and nonlinear optical processes on the nanoscale. This is a formidable problem because light can normally only be focused down to microscale regions due to the diffraction limit. Various schemes have been developed to couple laser radiation to the nanoscale, e.g., using tapered optical fibers or metal tips. Typically, only a small fraction of the incident energy can be transferred to the local field, and the rest is scattered as a stray background. Moreover, it is usually impossible to excite a single desired mode of the nanostructure. Several recently proposed schemes include using a tightly focused beam to improve the coupling of light with a nanoscale object [1,2], spatial and/or temporal shaping of the incident field to create subwavelength energy hot spots [3–7], and enhancing optical absorption by matching the shape of a nanoparticle to the field structure of a tightly focused beam [8]. While significant improvements are demonstrated in numerical simulations, perfect coupling or absorption is not possible with these approaches. In this Letter, we propose a method for full delivery of optical energy to individual resonances of subwavelength structures.

Our method is based on time-reversed lasing, or coherent perfect absorption (CPA), a generalization of the concept of critical coupling to a cavity, that has recently been developed and realized using a simple silicon cavity [9,10]. Any bounded optical system can be described by an electromagnetic scattering matrix, $\hat{S}$, which satisfies $\hat{S} \cdot \alpha = \beta$, where α, β are vectors of complex coefficients specifying the amplitudes of appropriate asymptotic incoming and outgoing states of the Maxwell wave equation. A threshold for lasing corresponds to the situation when $\epsilon(\vec{r})$, the full permittivity of the system including the gain medium, allows a solution with only outgoing waves, i.e., an eigenvalue of the S matrix tends to infinity for some frequency, ω_μ [9]. The time-reversed process to this lasing emission corresponds to imposing the phase-conjugated lasing mode on the system and changing gain to absorption, $\epsilon(\vec{r}) \rightarrow \epsilon^*(\vec{r})$; in this case β^* represents the incoming wave pattern and $\alpha^* \rightarrow 0$, there are no outgoing waves. Thus any system with resonances in a particular range of permittivity and frequency can be made to absorb perfectly a specific input electromagnetic radiation pattern by tuning to the lasing frequency (varying either the real part of the permittivity, ϵ_1, or the input frequency, ω) and simultaneously varying the material absorptivity (the imaginary part of the permittivity, ϵ_2) to be equal in magnitude (but opposite in sign) to the threshold gain. We refer to such a tunable lossy cavity as a coherent perfect absorber.

Subwavelength dielectric cavities cannot function as coherent perfect absorbers simply because they do not support resonances for wavelengths smaller than a half wavelength in the medium. However, metallic nanostructures support well-known surface plasmon resonances, and indeed recent work has demonstrated that composite metal-dielectric structures with gain can lase, such systems being termed ''spasers'' (surface plasmon amplification by stimulated emission) [11–16]. The cavity modes correspond to localized surface plasmon (LSP) resonances, which couple to light at the surface of the cavity, producing coherent emission. The complex conjugate index can be achieved in a purely metallic structure, since gain is not needed and the metal can provide the appropriate absorption; it then follows that the phase-conjugated ''spasing'' mode will be perfectly absorbed as an input. We are guaranteed perfect conversion of propagating waves from the far-field zone to the correct near-field pattern and finally to localized surface plasmons. This perfectly efficient excitation of LSPs in metallic nanostructures is accompanied by the creation of giant local fields, which may be useful for nanoscale linear and nonlinear optical probing and manipulation. The lack of scattered light suggests possible applications in background-free spectroscopy and microscopy. Furthermore, we will see that the CPA condition can be very sensitive to small changes in the environment, which points to applications in refractive index sensing and detection of small concentrations of target molecules.

The relationship of CPA to lasing makes it clear that it does not rely on any specific symmetry of the ''cavity,'' and

in its subwavelength application to plasmonic structures it can apply to nanoparticles of any shape or to clusters of nanoparticles, for which the CPA is the time-reverse of a random spaser. In these general cases the time-reversed lasing mode will be some complicated superposition of incoming cylindrical waves (2D case) or spherical waves (3D case). Here we will illustrate the effect for nanocylinders and nanospheres, for which angular momentum conservation guarantees a set of CPA resonances for each incident multipole field, and no superposition is necessary.

Consider an infinite metallic cylinder of radius R of complex permittivity $\epsilon = \epsilon_1 + i\epsilon_2$ (refractive index $n = \sqrt{\epsilon} = n_1 + in_2$) and axis along the z direction, embedded in a dielectric medium, of real and positive permittivity, $\epsilon_0 (n_0 = \sqrt{\epsilon_0})$. The incident light is assumed to propagate in the x-y plane, as does any scattered light. As noted, due to the cylindrical symmetry of the system, the axial component of angular momentum is conserved on scattering, as is the polarization. The scattering matrix is therefore diagonal, and its eigenstates, including the CPA eigenstates, with eigenvalue zero (no outgoing waves), can be labeled by azimuthal mode numbers, $m = 0, \pm 1, \pm 2, \ldots$, corresponding to a single multipole field. (Note that in this approach, assuming an incident angular momentum state, the scattered wave refers to the *entire* outgoing wave, as opposed to approaches based on plane wave illumination, in which the outgoing wave consists of both a scattered wave and an unscattered incident wave.) Incident fields with transverse magnetic (TM) polarization have electric fields in the x-y plane only, and can excite LSPs of the cylinder, leading to resonances. Incident fields with transverse electric polarization have electric field only in the z direction, cannot generate surface charge, and cannot excite LSPs. Thus we find CPA resonances exist only for TM modes. Moreover, if $\epsilon_1 > 0$, corresponding to a dielectric structure, then we find no subwavelength CPA resonances.

We determine the CPA resonances as follows. Outside the cylinder ($r > R$), the total magnetic field of a TM mode is

$$H_z(r, \theta, z) = H_m^{(2)}(n_0 kr) e^{im\theta} + s H_m^{(1)}(n_0 kr) e^{im\theta}, \quad (1)$$

where $n_0 = \sqrt{\epsilon_0}$, $k = 2\pi/\lambda$, and λ is the vacuum wavelength. $H_m^{(1)}$ [$H_m^{(2)}$] is the mth-order Hankel function of the first (second) kind, and represents an outgoing (incoming) wave. The complex number, s, is the relative amplitude of the outgoing wave for this mode (and also, in this case, the eigenvalue of the S matrix, since there is no interchannel scattering). Inside the metallic cylinder ($r < R$), the magnetic field is $H_z(r, \theta, z) = a J_m(nkr) e^{im\theta}$, where J_m is the Bessel function of the first kind, $n = \sqrt{\epsilon}$, and a is a normalization constant. By matching the fields at the metal or dielectric interface ($r = R$), we find

$$s = \frac{n J_m(nkR) H_m^{(2)\prime}(n_0 kR) - n_0 J_m'(nkR) H_m^{(2)}(n_0 kR)}{n_0 J_m'(nkR) H_m^{(1)}(n_0 kR) - n J_m(nkR) H_m^{(1)\prime}(n_0 kR)}, \quad (2)$$

where J' (H') is the first-order derivative of the Bessel (Hankel) function. For CPA resonance, the outgoing wave vanishes ($s = 0$), which corresponds to the condition

$$n J_m(nkR) H_m^{(2)\prime}(n_0 kR) = n_0 J_m'(nkR) H_m^{(2)}(n_0 kR). \quad (3)$$

Note that the lasing threshold would correspond to vanishing denominator ($s \to \infty$), which is just the complex conjugate condition. Equation (3) is the CPA condition for any uniform cylinder; as noted, only for a metallic cylinder, with $\epsilon_1 < 0$, can we obtain solutions with $kR \ll 1$.

Figure 1 plots the CPA solutions for dipole ($m = 1$) and quadrupole ($m = 2$) incident fields for a metallic cylinder with radius $R = 0.048\ \lambda$. Strong buildup of local fields is seen. The maximal enhancement of the electric field intensity via perfect coupling to the quadrupole resonance of LSP exceeds that of bow-tie or directional antennas with plane wave illumination [17,18]. Of course, the latter would have higher local field enhancement if the CPA condition is reached.

The same phenomenon can be realized in a metallic sphere. Again, LSP modes exist only for TM polarization (the radial component of the magnetic field vanishes). The CPA condition is obtained following procedures similar to the above and can be expressed as

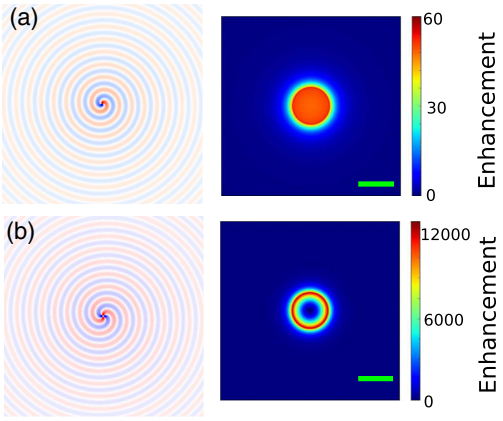

FIG. 1 (color online). Perfect coupling of incident waves to the dipole (a) and quadrupole (b) resonances of surface plasmons in a metallic nanocylinder. Left panels show the spatial distribution of the magnetic field H_z at an arbitrary time, showing that the incident wave spirals into the cylinder without any outgoing wave. For (a), $m = 1$ and $\epsilon = -1.14 + 0.158i$. For (b), $m = 2$ and $\epsilon = -1.03 + 0.00162i$. In both cases, $kR = 0.3$ and $\epsilon_0 = 1$. Right panels are an expanded view of the electric field intensity distribution in the vicinity of the cylinder. The stationary intensity pattern is obtained by averaging over one optical cycle, so the spiral pattern, which rotates in time, is smeared out. To show the enhancement factor, the field intensity is normalized by the maximal intensity of the incident field in the absence of the metallic cylinder. The scale bar is equal to the diameter of the cylinder.

$$\epsilon j_l(y_0)\frac{\partial[xh_l^{(2)}(x)]}{\partial x}\bigg|_{x=x_0} = \epsilon_0 h_l^{(2)}(x_0)\frac{\partial[yj_l(y)]}{\partial y}\bigg|_{y=y_0}, \quad (4)$$

where $x = \sqrt{\epsilon_0}kr$, $y = \sqrt{\epsilon}kr$, $x_0 = \sqrt{\epsilon_0}kR$, $y_0 = \sqrt{\epsilon}kR$, R is the radius of the metallic sphere, and ϵ and ϵ_0 are the permittivity of the metallic sphere and dielectric host medium, respectively. j_l is the lth-order spherical Bessel function, and $h_l^{(2)}$ the spherical Hankel function of the second kind.

We consider a metallic sphere in free space ($\epsilon_0 = 1.0$). As noted, in order to tune to CPA resonance, one must vary two parameters; here we fix the frequency and vary both the real and imaginary parts of ϵ, as in Ref. [9]. Instead of showing specific plasmonic CPA resonances at given values of kR, we show in Fig. 2 the continuous variation of the complex "CPA permittivity" under variation of kR, for two resonances with $l = 1$, 2. Indeed we find that plasmonic CPA resonances can be realized for an arbitrarily small metallic sphere. When $R \to 0$, $\epsilon_1 \to -2.0$ and $\epsilon_2 \to 0$ for $l = 1$. This corresponds to the quasistatic limit of the LSP resonance. For $l = 2$, $\epsilon_1 \to -1.5$, and again $\epsilon_2 \to 0$ as $R \to 0$. Both solutions have ϵ_2 vanishing in the quasistatic limit, because in this limit the radiative loss of the sphere is tending to zero, requiring very small absorptivity to reach critical coupling. Larger absorptivity actually decreases the total absorption.

Such low dissipative loss is not typically achievable for a solid metal nanoparticle. For example, when the dispersive permittivity of gold $\epsilon(k)$ [19] is inserted into Eq. (4), one finds that the smallest achievable value of kR is 0.91 at $\lambda = 535$ nm and $l = 2$. We therefore consider a composite silica core-gold shell structure, shown schematically in the inset of Fig. 3(a). The core sphere has radius R_c and the shell's outer radius is R. As the gold shell gets thinner, the fraction of metal decreases and the dissipative loss of the system is reduced. For a fixed ratio R_c/R, we vary k and R to find the CPA resonances (note that ϵ changes with k according to the dispersion relation of the gold). As shown in the main panel of Fig. 3(a), the minimum achievable value of kR for CPA decreases as R_c/R increases. At the same time, the LSP resonance shifts to longer wavelengths where the metal loss is lower. For example, when $R_c/R = 0.9$ and $R = 63$ nm, the CPA condition is reached at $\lambda = 771$ nm for $l = 1$. The near-field average intensity enhancement, defined as the electric field intensity averaged over the outer surface and divided by the maximal intensity of the incident light in the absence of the core-shell structure, is about 244. It is notably higher than the enhancement by tight focusing of a linearly or radially polarized beam [20] onto a gold sphere of similar size to excite the dipole LSP resonance [21,22].

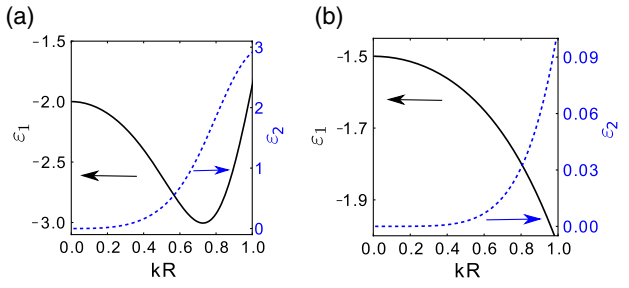

FIG. 2 (color online). CPA solution for a metallic sphere in free space. Real part (left vertical axis) and imaginary part (right vertical axis) of the permittivity of the metal as a function of kR for perfect coupling of impinging light to the LSP modes with $l = 1$ (a) and $l = 2$ (b). CPA is possible for an arbitrarily small sphere with finite values of refractive index and absorption coefficient.

It might appear that CPA cannot occur for dark ("non-radiative") plasmonic resonances. However, a typical dark mode only has a vanishing electric dipole moment; radiation can still occur in higher multipole moments (e.g. magnetic dipole and electric quadrupole). Hence, it is possible in principle to achieve CPA by coupling to a dark mode, as long as the radiative coupling of the dark mode is not completely vanishing; however, similar to the quasistatic limit, the high quality (Q) of the dark mode imposes the requirement of very low dissipation, which may be challenging to achieve.

In contrast to a spaser (or laser), perfect absorption based on time-reversed lasing can occur for any LSP resonance of the structure—not just the low-loss ones. Just as in a laser, the spaser usually oscillates in the LSP resonances with lowest loss, which saturates the gain, making it difficult for higher-loss resonances to reach threshold. The coherent perfect absorber is a linear device for which each resonance can be accessed independently by appropriate tuning of parameters.

The CPA phenomenon is extremely sensitive to variations in the incident wave or the dielectric environment. Small changes can violate the perfect-absorption condition, resulting in a dramatic increase of the scattered intensity. Figure 4 plots the scattered intensity of the outgoing wave, $|s|^2$, for a metallic cylinder as a function of the incoming light frequency k. As k deviates from a

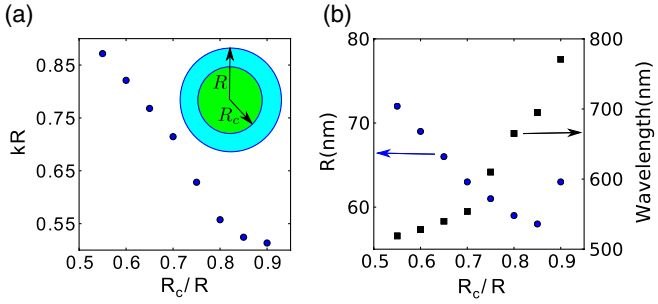

FIG. 3 (color online). CPA for silica core–gold shell structures. (a) Minimal value of kR as a function of R_c/R for $l = 1$. Inset: a schematic diagram of the core-shell structure. (b) Corresponding wavelength ($\lambda = 2\pi/k$) and radius R versus R_c/R.

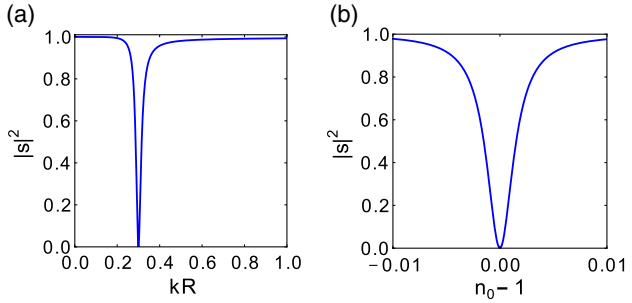

FIG. 4 (color online). Sensitivity of CPA to variations in the incident wave and the dielectric environment. (a) Normalized intensity $|s|^2$ of the outgoing wave versus the frequency k of the incident light (normalized by $1/R$, where R is the radius of the metallic cylinder). CPA is reached at $kR = 0.3$ via resonant excitation of the LSP resonance with $m = 2$. The spectral width of the dip in $|s|^2$ is determined by the dissipative loss of the LSP resonance. (b) $|s|^2$ as a function of the change in refractive index $n_0 - 1$ of the dielectric material surrounding the metallic cylinder. CPA happens at $n_0 = 1$. A tiny (less than 1%) deviation of n_0 from unity causes a dramatic growth of the scattered light intensity.

LSP resonance frequency, the scattered light intensity increases rapidly from zero. The spectral width of the CPA resonance is $\Delta k/k \simeq 0.1$, and it is determined by the dissipative loss of the LSP mode. This result is promising for application to background-free spectroscopy. A similar effect is found for a tiny change in refractive index or absorption coefficient of the surrounding material, as shown in Fig. 4(b) for a variation in n_0. Hence, the effect may be useful for ultrasensitive detection of environmental changes. The high sensitivity also means that some sort of adaptive scheme [6,7,23,24] would be needed to produce the correct incident wave front if the surrounding is not perfectly homogeneous.

In the recent development of metamaterial absorbers, impedance matching has been used to eliminate reflection of a plane wave from the front surface, with transmission minimized by the use of multiple absorbing layers or a mirror at the back surface of the sample [25–29]. Although the dimension of each unit cell is subwavelength, the entire medium is macroscopic. Also perfect conversion of an electromagnetic wave to the surface plasmon polariton has been realized with a bulk plasma by placing a subwavelength grating in front of the plasma surface [30,31]. CPA, which can be regarded as a generalization of the concept of impedance matching to arbitrary geometries and dimension, is applied here to a single subwavelength object in free space. By matching the incident field pattern to the radiation pattern of a LSP resonance, 100% coupling efficiency is reached. However, the input field for perfect coupling to a nanosphere is an angular momentum eigenstate, which must converge onto it from all directions, something not easily realized experimentally. To simplify the experimental requirements, it will likely be useful to strongly break the rotation symmetry, e.g., by employing ellipsoids or nanorods, in order to approach the resonance condition with a more directional input wave pattern.

The CPA mechanism differs from another application of the time-reversal principle to the spatial-temporal localization of optical energy in a nanoplasmonic system [4]. In the latter case, a short pulse is launched from a point in the near field and the radiation in the far field is recorded. Time-reversal of the radiated pulse leads to concentration of input energy at the position of the initial source at a time corresponding to the end of the excitation pulse, and afterward the field passes through the focal point and diverges. This effect is not based on intrinsic resonances of the nanostructure and the input energy is not completely absorbed at the focus, unless a time-reversed source (sink) is placed there [32]. In contrast, the CPA sets up a perfect "trap" for the incident light by matching it to a resonance of the system. Thus it works only for coherent light at the resonance frequencies, but does not require a coherently driven sink.

In summary, we have demonstrated the possibility of coherent perfect absorption of light by nanoscale metallic objects, equivalent to time-reversing the spaser and perfect coupling to localized surface plasmons. Such perfect absorption is fundamentally different from the optical cloaking [33,34] that has been extensively investigated in recent years. For optical cloaking the impinging field is rerouted and appears as an unscattered outgoing wave, whereas in the CPA there *are* no outgoing waves, for a certain input field the nanostructure appears "black" (in a narrow band), but not invisible.

We thank Professors Mathias Fink, Geoffroy Lerosey, and Rupert F. Oulton for stimulating discussions. This work is funded by the NSF Grant No. DMR-0908437 and No. ECCS-1068642.

*hui.cao@yale.edu

[1] G. Zumofen, N. M. Mojarad, V. Sandoghdar, and M. Agio, Phys. Rev. Lett. **101**, 180404 (2008).
[2] N. M. Mojarad, V. Sandoghdar, and M. Agio, J. Opt. Soc. Am. B **25**, 651 (2008).
[3] M. I. Stockman, S. V. Faleev, and D. J. Bergman, Phys. Rev. Lett. **88**, 067402 (2002).
[4] X. Li and M. I. Stockman, Phys. Rev. B **77**, 195109 (2008).
[5] A. Sentenac and P. C. Chaumet, Phys. Rev. Lett. **101**, 013901 (2008).
[6] G. Volpe, G. Molina-Terriza, and R. Quidant, Phys. Rev. Lett. **105**, 216802 (2010).
[7] T. S. Kao, S. D. Jenkins, J. Ruostekoski, and N. I. Zheludev, Phys. Rev. Lett. **106**, 085501 (2011).
[8] A. Normatov, B. Spektor, Y. Leviatan, and J. Shamir, Opt. Express **19**, 8506 (2011).
[9] Y. D. Chong, L. Ge, H. Cao, and A. D. Stone, Phys. Rev. Lett. **105**, 053901 (2010).

[10] W. Wan, Y. Chong, L. Ge, H. Noh, A. D. Stone, and H. Cao, Science **331**, 889 (2011).
[11] D. J. Bergman and M. I. Stockman, Phys. Rev. Lett. **90**, 027402 (2003).
[12] N. I. Zheludev, L. S. Prosvirnin, N. Papasimakis, and A. V. Fedotov, Nature Photon. **2**, 351 (2008).
[13] M. A. Noginov, G. Zhu, A. M. Belgrave, R. Bakker, V. M. Shalaev, E. E. Narimanov, S. Stout, E. Herz, T. Suteewong, and U. Wiesner, Nature (London) **460**, 1110 (2009).
[14] R. F. Oulton, V. J. Sorger, T. Zentgraf, R.-M. Ma, C. Gladden, L. Dai, G. Bartal, and X. Zhang, Nature (London) **461**, 629 (2009).
[15] M. I. Stockman, Phys. Rev. Lett. **106**, 156802 (2011).
[16] S. Wuestner, A. Pusch, K. L. Tsakmakidis, J. M. Hamm, and O. Hess, Phys. Rev. Lett. **105**, 127401 (2010).
[17] P. J. Schuck, D. P. Fromm, A. Sundaramurthy, G. S. Kino, and W. E. Moerner, Phys. Rev. Lett. **94**, 017402 (2005).
[18] P. Muhlschlegel, H.-J. Eisler, O. J. F. Martin, B. Hecht, and D. W. Pohl, Science **308**, 1607 (2005).
[19] P. B. Johnson and R. W. Christy, Phys. Rev. B **6**, 4370 (1972).
[20] S. Quabis, R. Dorn, M. Eberler, O. Glckl, and G. Leuchs, Opt. Commun. **179**, 1 (2000).
[21] N. M. Mojarad, V. Sandoghdar, and M. Agio, J. Opt. Soc. Am. B **25**, 651 (2008).
[22] N. M. Mojarad and M. Agio, Opt. Express **17**, 117 (2009).
[23] I. M. Vellekoop and A. P. Mosk, Opt. Lett. **32**, 2309 (2007).
[24] B. Gjonaj, J. Aulbach, P. M. Johnson, A. P. Mosk, L. Kuipers, and A. Lagendijk, Nature Photon. **5**, 360 (2011).
[25] N. I. Landy, S. Sajuyigbe, J. J. Mock, D. R. Smith, and W. J. Padilla, Phys. Rev. Lett. **100**, 207402 (2008).
[26] Y. Avitzour, Y. A. Urzhumov, and G. Shvets, Phys. Rev. B **79**, 045131 (2009).
[27] B. Wang, T. Koschny, and C. M. Soukoulis, Phys. Rev. B **80**, 033108 (2009).
[28] N. Liu, M. Mesch, T. Weiss, M. Hentschel, and H. Giessen, Nano Lett. **10**, 2342 (2010).
[29] A. Polyakov, S. Cabrini, S. Dhuey, B. Harteneck, P. J. Schuck, and H. A. Padmore, Appl. Phys. Lett. **98**, 203104 (2011).
[30] Y. P. Bliokh, J. Felsteiner, and Y. Z. Slutsker, Phys. Rev. Lett. **95**, 165003 (2005).
[31] Y. P. Bliokh, Y. L. Brodsky, K. B. Chashka, J. Felsteiner, and Y. Z. Slutsker, Phys. Plasmas **17**, 083302 (2010).
[32] J. de Rosny and M. Fink, Phys. Rev. Lett. **89**, 124301 (2002).
[33] U. Leonhardt and D. R. Smith New J. Phys. **10**, 115019 (2008).
[34] *Applications of Metamaterials, Metamaterials Handbook*, edited by F. Capolino (CRC Press, Boca Raton, FL, 2009).